Robotica (2012) volume 30, pp. 635–648. © Cambridge University Press 2011
doi:10.1017/S0263574711000671

Optimal mapping of joint faults into healthy joint velocity space for fault-tolerant redundant manipulators

Hamid Abdi*,†,‡, Saeid Nahavandi†, Yakov Frayman† and Anthony A. Maciejewski‡

†*Centre for Intelligent Systems Research (CISR), Deakin University, Waurn Ponds Campus, VIC 3217, Australia.*
E-mails: {hamid.abdi, saeid.nahavandi, yakov.frayman}@deakin.edu.au
‡*Electrical and Computer Engineering Department, Colorado State University, Fort Collins, CO 80523, USA.*
E-mail: aam@colostate.edu

(Accepted June 9, 2011. First published online: August 8, 2011)

SUMMARY
Self-reconfiguration of robotic manipulators under joint failure can be achieved via fault-tolerance strategies. Fault-tolerant manipulators are required to continue their end-effector motion with a minimum velocity jump, when failures occur to their joints. Optimal fault tolerance of the manipulators requires a framework that can map the velocity jump of the end-effector to the compensating joint velocity commands. The main objective of the present paper is to propose a general framework for the fault tolerance of the manipulators, which can minimize the end-effector velocity jump. In the present paper, locked joint failures of the manipulators are modeled using matrix perturbation methodology. Then, the optimal mapping for the faults with a minimum end-effector velocity jump is presented. On the basis of this mapping, the minimum end-effector velocity jump is calculated. A generalized framework is derived from the extension of optimal mapping toward multiple locked joint failures. Two novel expressions are derived representing the generalized optimal mapping framework and the generalized minimum velocity jump. These expressions are suitable for the optimal fault tolerance of the serial link redundant manipulators. The required conditions for a zero end-effector velocity jump of the manipulators are analyzed. The generalized framework in this paper is then evaluated for different failure scenarios for a 5-DOF planar manipulator and a 5-DOF spatial manipulator. The validation includes three case studies. While the first two are instantaneous studies, the third one is for the whole trajectory of the manipulators. From the results of these case studies, it is shown that, when locked joint faults occur, the faulty manipulator is able to optimally maintain its velocity with a zero end-effector velocity jump if the conditions of a zero velocity jump are hold.

KEYWORDS: Robotic manipulators; Optimal fault tolerance; Optimal joint velocity; Actuator failures; Redundancy resolution; Dependability; Self-reconfiguration.

* Corresponding author. E-mail: hamid.abdi@deakin.edu.au

1. Introduction

Fault-tolerant manipulators are essential wherever high dependability of robots is required, such as robotic manipulators applied in hazardous environments. The application might be nuclear disposal, deep-sea missions, or outer-space explorations.[1,2] This fact has been noticed for the teleoperated manipulators for handling of hazardous or explosive chemicals.[3,4] Design and control of fault-tolerant manipulator aim to maintain the dependability of the manipulator despite of partial failures. The fault might occur in the actuators or the sensors of the manipulator.[5,6]

Research on fault tolerance of the manipulators is on either the design of the manipulators (design of fault-tolerant manipulators or fault-tolerant structures) or the control of the manipulators (fault analysis and fault-tolerant motion planning or control). Within the literature of design of fault-tolerant manipulators, either different structure of serial or parallel manipulators have been studied,[7–12] or a manipulator with a specific fault-tolerant property has been designed that includes design of degrees of freedom (DOF), link lengths, and redundancy in actuation.[13,14] The design procedure usually optimizes fault-tolerance measures of the manipulators.[12,14] For instance, relative manipulability[15] or worst-case dexterity[16] are two of measures of fault tolerance of manipulators. Condition number of manipulators can also be used for the fault tolerance, this fact has been observed in our previous work[17] where the condition numbers are used for finding optimal configurations for fault tolerance of the manipulator. In the literature of the fault-tolerant control of the manipulators, subjects, such as fault detection, fault isolation, fault identification, and fault accommodation of the manipulators, are studied.[18–21]

Serial link manipulators (SLMs) have received a great level of attention by the researchers in the robotics community. Fault-tolerant design of the SLMs can be achieved by adding extra kinematic redundancy to the manipulators. A SLM with extra kinematic redundancy is called serial link redundant manipulator (SLRM).[11,22,23] Via these kinematic redundancies, the manipulator can be dependable to perform a required[24] or prioritized tasks[25] despite of the joint failures. The added kinematic redundancy not only improves the fault tolerance of the manipulators, but also promotes other static or dynamic properties of the manipulators. These properties can be used for higher dexterous movements,[26] lower maintenance and repair costs, obstacle avoidance, and so on. In fact, SLRMs have the capability to be used under multiple constraints.[25,27,28] Keeping in mind that having kinematic redundancy does not guarantee the fault tolerance for the operation of SLRMs, because the redundancy has to be effectively used for fault tolerance[29] of SLRMs.

Self-X systems are systems with self-assembly, self-organization, self-reconfiguration, self-repair, self-replication, or self-reproduction capability.[30] The problem of self-joint-velocity reconfiguration for robotic manipulators under locked joint failures is addressed in the present paper. The reconfiguration is proposed for locked joint failures via incorporating fault-tolerance strategies. When a locked joint failure occurs, it will cause an end-effector (EEF) velocity jump because the locked joint stops to contribute into the velocity of the EEF. The fault-tolerant manipulators are expected to continue their motion tasks with a minimum EEF velocity jump when faults occur into their joints. For having this property, the contribution of the locked joints prior to the fault time has to be compensated by healthy joints via a proper reconfiguration strategy. This reconfiguration requires a framework to map the EEF velocity jumps to the compensating velocity commands for the healthy joints. The compensating velocity commands must be calculated in a way that optimally recovers EEF velocity jump.

While the focus of the present work is on the EEF velocity jump, number of the literature has discussed the joint velocity jump (JVJ), such as the studies in refs. [31, 32]. The mapping in refs. [31, 32] is based on minimization of the minimum JVJ. The focus in the present paper is the minimum EEF velocity jump. The work in refs. [31, 32] obtained minimum JVJ by using Lagrange multiplier method for the velocity equation of the faulty manipulator and reported only a single joint failure. But the present work is using least-square technique within the methodology of matrix perturbation. In fact, the perturbation methodology provides a better interpretation of the optimal mapping and is very suitable for the extension toward multiple locked joint failures.

The present paper is organized as following: At first, the velocity equation of SLRMs with locked joint failure is introduced with matrix perturbation methodology. Then, the minimum EEF velocity jump is obtained, which gives an optimal mapping for the fault tolerance of the SLRMs. From this fault-tolerance mapping, the required conditions to have a zero EEF velocity jump are analyzed. Next, the mapping is extended toward multiple locked joint failures and a generalized framework for optimal fault tolerance with minimum EEF velocity jump is indicated. Finally, three case studies are implemented to validate the proposed fault-tolerance framework.

2. Kinematics of Serial Link Redundant Manipulators

In this section, kinematics of SLRMs with locked joints failures is established. Within the formulas throughout this paper, the capital letters represent matrices and small letters represent vectors or scalar parameters. The matrices are assumed to be full rank. If the number of the columns of matrices is greater than the rows, then they are called fat matrix and if it is less, they are called skinny matrix.

2.1. Kinematic and self-motion manifolds

Fault-tolerant analysis of robotic manipulators studies different redundancies of the manipulators for the sake of fault tolerance. The forward kinematics of a multirigid body is introduced as a base of fault-tolerance analysis

$$\mathbf{x} = \mathbf{f}(\mathbf{q}), \tag{1}$$

$$\mathbf{q} = [q_1 \quad q_2 \quad \dots \quad q_n]^{\mathrm{T}}, \tag{2}$$

$$\mathbf{x} = [x_1 \quad x_2 \quad \dots \quad x_m]^{\mathrm{T}}, \tag{3}$$

where $\mathbf{f} : R^n \to R^m$ is the forward kinematic function of the manipulators and it is a nonlinear equation. The manipulators in this paper are assumed to be revolute joint manipulators. Forward kinematics relates joint angles (2) to EFF positional and orientational variables (3).

The joint variables define the configuration space (C-space), and positional and orientational variables define the work space of the manipulator. Knowing that $\mathbf{f} : R^n \to R^m$ then the manipulator has n-DOF, and n is the dimension of the C-space or joint space and m is called the dimension of the workspace. The degree of kinematic redundancy (DOR) in nonsingular kinematic configurations of the manipulators is obtained by $n - m$.

In ref. [13], the number of required redundancy was investigated by applying joint fault probability and total reliability of manipulators. In ref. [33], the upper limit of an optimal fault-tolerant configuration for redundant manipulators has been studied and it has indicated that the optimal fault-tolerant configuration is not possible for manipulators with more than 12-DOR. In general, the higher the degree of redundancy, the better fault tolerance of the manipulators. However, higher DOR for the manipulator may not result to an optimal fault tolerance of the manipulators. Identifying the fault-tolerant workspace of SLRMs requires a general solution of inverse kinematics equation

$$\mathbf{q} = \mathbf{f}^{-1}(\mathbf{x}). \tag{4}$$

For SLRMs, it is very rarely possible to find the general fault-tolerant workspace of the manipulator because of the redundancy of the solutions and the nonlinearity of Eq. (1). The work in refs. [34, 35] has introduced the concept of self-motion manifolds for the inverse kinematic problem of SLRMs. The characterizations of the self-motion manifolds, both in C-space and work space have been used for the fault-tolerance study of the manipulators.[34,35] The papers have applied manifold techniques to determine manifold solution for the inverse kinematic equations. Then, they have used them to obtain the fault-tolerant configurations of a manipulator. This type of analysis has very limited performance, especially from generalization point of view. Therefore, other methods for fault-tolerance study are preferred.

In last two decades, the fault tolerance of SLRMs has been widely addressed by the researchers in the robotics community. Recent work uses the properties of the Jacobian matrix or null space of the Jacobian matrix to define fault-tolerance measures or provide fault-tolerance control. For instance, some properties of the Jacobian matrix for fault tolerance have been used in refs. [14, 29]. The relationship between the fault tolerance and the null space of Jacobian matrix has been addressed.[29] Those measures of the fault tolerance are based on the Jacobian not only can be used for the design of the manipulators, but also they can be used for the fault tolerance in the operation of the manipulators. This motivates the use of Jacobian matrix for the fault-tolerant motion of manipulators.

2.2. *Jacobian matrix of SLRMs with locked joint faults*

The Jacobian matrix of manipulators is shown as

$$\mathbf{J} = \left[\frac{\partial \mathbf{f}}{\partial \mathbf{q}}\right] \in R^{m\times n}. \tag{5}$$

Jacobian matrix relates the EFF translational and orientational velocity to the joint velocities

$$\dot{\mathbf{x}} = \mathbf{J}\dot{\mathbf{q}}, \tag{6}$$

where $\mathbf{J} = [\mathbf{j}_1 \ \dots \ \mathbf{j}_{k-1} \ \mathbf{j}_k \ \mathbf{j}_{k+1} \ \dots \ \mathbf{j}_n]$ and $\mathbf{j}_k \in R^m$ is the kth column of $\mathbf{J}$. The velocity equation (6) can be written as

$$\dot{\mathbf{x}} = \sum_{k=1}^{n} \mathbf{j}_k \dot{q}_k. \tag{7}$$

Physically, $\mathbf{j}_k$ in Eq. (7) indicates the contribution of the kth joint velocity to the translational and orientational velocity of the EEF. Normally, we have $n \geq m$ that is for a square or fat matrix and in nonkinematic singular configurations of the manipulators, the rank of the Jacobian matrix is m. The common modeling method for the locked joint failures of the manipulators in the literature[14,36,37] is presented in following.

When the manipulator has a fault in its kth joint, then it stops to contribute to the velocity of EFF of the manipulator. Therefore, the Jacobian matrix of the faulty manipulator with a locked joint failure is introduced by replacing a zero vector in the kth column of the Jacobian matrix, which gives

$$[\mathbf{j}_1 \ \dots \ \mathbf{j}_{k-1} \ \ 0 \ \ \mathbf{j}_{k+1} \ \dots \ \mathbf{j}_n]. \tag{8}$$

This Jacobian matrix is reduced to a matrix, which is called kth reduced Jacobian matrix as

$${}^{k}\mathbf{J} = [\mathbf{j}_1 \ \dots \ \mathbf{j}_{k-1} \ \ \mathbf{j}_{k+1} \ \dots \ \mathbf{j}_n] \in R^{m\times(n-1)}. \tag{9}$$

The kth reduced Jacobian matrix is obtained simply by eliminating the kth column of Eq. (5). The velocity equation of faulty manipulator with a single locked joint fault is obtained then by

$$\dot{\mathbf{x}} = {}^{k}\mathbf{J}^{k}\dot{\mathbf{q}}, \tag{10}$$

where

$${}^{k}\dot{\mathbf{q}} = [\dot{q}_1 \ \dots \ \dot{q}_{k-1} \ \ \dot{q}_{k+1} \ \dots \ \dot{q}_n]^{\mathrm{T}} \in R^{n-1}. \tag{11}$$

Here, the vector ${}^{k}\dot{\mathbf{q}}$ is the joint velocity vector of the reduced manipulator. For single joint failures of n-DOF manipulators, there are m number of reduced Jacobian matrices as

$$\{{}^{1}\mathbf{J}, {}^{2}\mathbf{J}, \dots, {}^{n}\mathbf{J}\}, \tag{12}$$

where ${}^{k}\mathbf{J}$ is the kth reduced Jacobian matrix that is due to the fault of the kth joint.

Knowing that $n \geq m$, then the matrix ${}^{k}\mathbf{J}$ is a skinny matrix when $\mathbf{J}$ is square. The matrix ${}^{k}\mathbf{J}$ is square when $n = m + 1$ or manipulator has only 1-DOR; otherwise, when $n > m + 1$ then ${}^{k}\mathbf{J}$ is a fat matrix.

With a similar approach, if a manipulator has r faults, then the Jacobian matrices of faulty manipulator are obtained by the permutation of r zero vectors in the original Jacobian matrix. In general, with $r, r = 1, \dots, n$ faults, there are $\binom{n}{r} = \frac{n!}{r!(n-r)!}$ reduced Jacobian matrices. For instance, if two faults occur into the joints of k and l when $k, l = 1, \dots, n$ and $k < l$, then there are $\frac{n(n-1)}{2}$ reduced Jacobian matrices indicated as

$${}^{k,l}\mathbf{J} = [\mathbf{j}_1 \ \dots \ \mathbf{j}_{k-1} \ \mathbf{j}_{k+1} \ \dots \ \mathbf{j}_{l-1} \ \mathbf{j}_{l+1} \ \dots \ \mathbf{j}_n] \in R^{m\times(n-2)}. \tag{13}$$

The velocity equation for manipulators with two locked joints is written as

$$\dot{\mathbf{x}} = {}^{k,l}\mathbf{J}^{k,l}\dot{\mathbf{q}} \quad k, l = 1, \dots, n \quad k < l, \tag{14}$$

$${}^{k,l}\dot{\mathbf{q}} = [\dot{q}_1 \ \dots \ \dot{q}_{k-1} \ \dot{q}_{k+1} \ \dots \ \dot{q}_{l-1} \ \dot{q}_{l+1} \ \dots \ \dot{q}_n]^{\mathrm{T}} \in R^{n-2}. \tag{15}$$

In general, for $r > 1$ faults, if $S_r = \{i_1\, i_2 \dots i_r |\ i_1 < i_2 < \dots < i_r \ 1 \leq i_1, i_r \leq n\}$ is the ascending set of faulty joints, then the velocity equation for a manipulator with r faults of S_r is represented by

$$\dot{\mathbf{x}} = {}^{S_r}\mathbf{J}^{S_r}\dot{\mathbf{q}}, \tag{16}$$

where ${}^{S_r}\mathbf{J}$ is obtained by eliminating the columns of $\mathbf{J}$ associated to the faulty joints, and ${}^{S_r}\dot{\mathbf{q}}$ is obtained by eliminating the corresponding rows from $\dot{\mathbf{q}}$. By this elimination, the matrix ${}^{S_r}\mathbf{J}$ will be a skinny matrix when $n < m + r$. The matrix ${}^{k}\mathbf{J}$ will be square matrix when $n = m + r$; otherwise, when $n > m + r$ then ${}^{k}\mathbf{J}$ will be a fat matrix.

3. Minimum Velocity Jump for Faulty Manipulator

3.1. *Matrix perturbation and single locked joint faults*

If a sudden locked failure occurs into the kth joint of a manipulator while the joint velocity expected to be $\dot{q}_k$ for the motion task, then the fault can be modeled via a perturbation in the velocity equation (6) as

$$\dot{\mathbf{x}} + \Delta\dot{\mathbf{x}} = (\mathbf{J} + \Delta\mathbf{J})(\dot{\mathbf{q}} + \Delta\dot{\mathbf{q}}), \tag{17}$$

where $\Delta\dot{\mathbf{x}}$ is the EEF velocity jump, $\Delta\mathbf{J}$ is the perturbation into the Jacobian matrix due to the failure, and $\Delta\dot{\mathbf{q}}$ is the joint velocities jump.

If the kth joint is locked, then the perturbation in the Jacobian matrix is

$$\Delta\mathbf{J} = \begin{bmatrix} 0 & \dots & -\mathbf{j}_k & \dots & 0 \end{bmatrix}. \tag{18}$$

Additionally, as the kth joint stops after failure, the joint velocities jump is

$$\Delta\dot{\mathbf{q}} = \begin{bmatrix} 0 & \dots & -\dot{q}_k & \dots & 0 \end{bmatrix}^{\mathrm{T}}, \tag{19}$$

where $\dot{q}_k$ is the expected velocity of the kth joint when the manipulator is healthy.

The perturbation approach here is consistent with the modeling in previous section. For the fault-tolerant manipulators, a control input is required to compensate the EEF velocity jump. Let assume $\mathbf{u}$ is the vector of the control input to compensate the failure of the kth joint of the manipulator. Adding this control input to Eq. (17) results in

$$\dot{\mathbf{x}} + \Delta\dot{\mathbf{x}} = (\mathbf{J} + \Delta\mathbf{J})(\dot{\mathbf{q}} + \Delta\dot{\mathbf{q}} + \mathbf{u}). \tag{20}$$

Using Eq. (6) to simplify Eq. (20) results in

$$\Delta\dot{\mathbf{x}} = (\mathbf{J} + \Delta\mathbf{J})\Delta\dot{\mathbf{q}} + \Delta\mathbf{J}\dot{\mathbf{q}} + (\mathbf{J} + \Delta\mathbf{J})\mathbf{u}. \tag{21}$$

Considering that $\mathbf{J} + \Delta\mathbf{J}$ is a matrix with zero vector in its kth column, and $\Delta\dot{\mathbf{q}}$ (19) is a zero vector except in the kth row, then $(\mathbf{J} + \Delta\mathbf{J})\Delta\dot{\mathbf{q}} \equiv 0$ and Eq. (21) results in

$$\Delta\dot{\mathbf{x}} = \Delta\mathbf{J}\dot{\mathbf{q}} + (\mathbf{J} + \Delta\mathbf{J})\mathbf{u}. \tag{22}$$

Using Eq. (18) in Eq. (22) obtains the velocity jump of the EEF as

$$\Delta\dot{\mathbf{x}} = -\mathbf{j}_k\dot{q}_k + (\mathbf{J} + \Delta\mathbf{J})\mathbf{u}. \tag{23}$$

Physically, Eq. (23) implies that the velocity jump at the EEF is equal to the lost contribution of the kth joint velocity $(-\mathbf{j}_k\dot{q}_k)$ plus the contribution of the compensating velocity of the other joints $(\mathbf{J} + \Delta\mathbf{J})\mathbf{u}$. Having zero in the kth column of $(\mathbf{J} + \Delta\mathbf{J})$ will ensure that $(\mathbf{J} + \Delta\mathbf{J})\mathbf{u}$ cancels any control command on the velocity of the kth joint. The faulty joint is a locked joint and the calculated joint velocity vector $\mathbf{u}$ must have a zero component in its kth row.

3.2. *Minimization of the EEF velocity jump subjected to a single joint fault*

This control input is obtained in a way to optimally maintain the velocity of the EEF, despite of the failure. Therefore, an optimality problem can be defined based on minimum EEF velocity jump for the velocity of the EEF after the failure. The norm of the EEF velocity jump is used for this minimization. The norm is

$$\|\Delta\dot{\mathbf{x}}\|^2 = \Delta\dot{\mathbf{x}}^{\mathrm{T}}\Delta\dot{\mathbf{x}} = (\Delta\mathbf{J}\dot{\mathbf{q}} + (\mathbf{J} + \Delta\mathbf{J})\mathbf{u})^{\mathrm{T}}(\Delta\mathbf{J}\dot{\mathbf{q}} + (\mathbf{J} + \Delta\mathbf{J})\mathbf{u}). \tag{24}$$

This norm can be used for minimization of the EEF velocity jump to obtain the optimal control input of $\mathbf{u}$. In the optimal case, the velocity jump is zero $\|\Delta\dot{\mathbf{x}}\| = 0$. This optimum case requires the vector of the EEF velocity jump to be zero $\Delta\dot{\mathbf{x}} = 0$ and by substituting to Eq. (23)

$$(\mathbf{J} + \Delta\mathbf{J})\mathbf{u}^{\mathrm{opt}} = \mathbf{j}_k\dot{q}_k, \tag{25}$$

where $\mathbf{u}^{\mathrm{opt}}$ is the optimal control input for joint velocities to minimize the EEF velocity jump. Expansion of Eq. (25) is

$$\begin{cases} j_{11}u_1 + \dots + j_{1(k-1)}u_{k-1} + j_{1(k+1)}u_{k+1} + \dots + j_{1n}u_n = j_{1k}\dot{q}_k, \\ \quad\cdots \\ j_{i1}u_1 + \dots + j_{i(k-1)}u_{k-1} + j_{i1(k+1)}u_{k+1} + \dots + j_{in}u_n = j_{ik}\dot{q}_k, \\ \quad\cdots \\ j_{m1}u_1 + \dots + j_{m(k-1)}u_{k-1} + j_{m(k+1)}u_{k+1} + \dots + j_{mn}u_n = j_{mk}\dot{q}_k. \end{cases} \tag{26}$$

Using the reduced Jacobian matrix in Eq. (9), and defining the reduced control input as ${}^k\mathbf{u} = [{}^ku_1 \;\; {}^ku_2 \;\; \dots {}^ku_{k-1} \; {}^ku_{k+1} \;\; \dots {}^ku_n\,]^{\mathrm{T}}$, Eq. (26) is encapsulated in

$${}^k\mathbf{J}\,{}^k\mathbf{u}^{\mathrm{opt}} = \mathbf{j}_k\dot{\mathbf{q}}_k. \tag{27}$$

${}^k\mathbf{u}^{\mathrm{opt}}$ is same as $\mathbf{u}^{\mathrm{opt}}$ except the kth row has been eliminated.

Equation (27) means that the optimal joint velocity must provide the same contribution to the velocity of the EEF as that of the lost contribution of the faulty joint. By comparing Eqs. (25) and (27), then $(\mathbf{J} + \Delta\mathbf{J})\mathbf{u}^{\mathrm{opt}} = {}^k\mathbf{J}\,{}^k\mathbf{u}^{\mathrm{opt}}$ and using this property in the norm of the velocity jump (24) results in

$$\|\Delta\dot{\mathbf{x}}\|^2 = (-\mathbf{j}_k\dot{q}_k + {}^k\mathbf{J}\,{}^k\mathbf{u}^{\mathrm{opt}})^{\mathrm{T}}(-\mathbf{j}_k\dot{q}_k + {}^k\mathbf{J}\,{}^k\mathbf{u}^{\mathrm{opt}}). \tag{28}$$

Equation (28) is then optimally solved by using least-square technique as

$${}^k\mathbf{u}^{opt} = ({}^k\mathbf{J})^{\dagger}\mathbf{j}_k\dot{q}_k, \tag{29}$$

where $({}^k\mathbf{J})^{\dagger}$ is Penrose–Moore or the pseudoinverse of ${}^k\mathbf{J}$. This pseudoinverse is only defined for nonsingular configuration of the faulty manipulators that is equivalent to the full rank of reduced Jacobian matrices. If the matrix ${}^k\mathbf{J}$ is a fat and full-rank matrix, then the pseudoinverse is obtained via right inverse of ${}^k\mathbf{J}$ by

$$({}^k\mathbf{J})^{\dagger} = ({}^k\mathbf{J})^{\mathrm{T}}(({}^k\mathbf{J})({}^k\mathbf{J})^{\mathrm{T}})^{-1}. \tag{30}$$

If ${}^k\mathbf{J}$ is a square and full-rank matrix, then $({}^k\mathbf{J})^{\dagger} = ({}^k\mathbf{J})^{-1}$.

If matrix ${}^k\mathbf{J}$ becomes skinny matrix and full rank, then the pseudoinverse is defined via left inverse of ${}^k\mathbf{J}$ as

$$({}^k\mathbf{J})^{\dagger} = (({}^k\mathbf{J})^{\mathrm{T}}\,{}^k\mathbf{J})^{-1}({}^k\mathbf{J})^{\mathrm{T}}. \tag{31}$$

Finally, by replacing pseudoinverse in Eq. (29), the control input vector is obtained. Then, by reconstructing $\mathbf{u}^{\mathrm{opt}}$ from its reduced form of ${}^k\mathbf{u}^{\mathrm{opt}}$, which can be done by adding a zero row to the kth row of ${}^k\mathbf{u}^{\mathrm{opt}}$ as

$$\mathbf{u}^{\mathrm{opt}} = \begin{bmatrix} {}^ku_1^{\mathrm{opt}} & \dots & {}^ku_{k-1}^{\mathrm{opt}} & 0 & {}^ku_k^{\mathrm{opt}} & \dots & {}^ku_{n-1}^{\mathrm{opt}} \end{bmatrix}^{\mathrm{T}}. \tag{32}$$

This is the vector of the optimal control input for the healthy joints. This input optimally compensates the EEF velocity jump when a fault occurs to the kth joint of the manipulator. Equations (29) and (32) provide a framework

https://doi.org/10.1017/S0263574711000671 Published online by Cambridge University Press

for optimal mapping of the loss contribution of the faulty joint ($\mathbf{j}_k\dot{q}_k$) to the compensating joint velocity of the healthy joints ($\mathbf{u}^{\text{opt}}$). This framework can be used when a fault occurs in the kth joint of the manipulator. For other joint failures and if $\mathbf{u}^{\text{opt}}$ is obtained for each the other joints, then a square matrix $\mathbf{V} \in R^{nn}$ can be defined form each $\mathbf{u}^{\text{opt}}$ as its column. This matrix includes the optimal control input of Eq. (32) for any single locked joint of an n-DOF manipulator and it can be used for the fault tolerance of any single locked joint failures of the manipulator. A method to compute $\mathbf{V}$ is to define a matrix $\mathbf{W} \in R^{n\times(n-1)}$ as

$$\mathbf{W} = [\mathbf{w}_1 \quad \mathbf{w}_2 \quad \dots \quad \mathbf{w}_n], \qquad (33)$$

where $\mathbf{w}_k$ is the kth column of $\mathbf{W}$ and each column is obtained by $\mathbf{w}_k = {}^k\mathbf{u}^{\text{opt}} = ({}^k\mathbf{J})^{\dagger}\mathbf{j}_k\dot{\mathbf{q}}_k$ when $k = 1, \dots, n$. The closed form of matrix $\mathbf{W}$ is

$$\mathbf{W} = \left[({}^1\mathbf{J})^{\dagger}\mathbf{j}_1 \quad ({}^2\mathbf{J})^{\dagger}\mathbf{j}_2 \quad \dots \quad ({}^n\mathbf{J})^{\dagger}\mathbf{j}_n\right]\text{diag}(\dot{\mathbf{q}}), \qquad (34)$$

where diag($\dot{\mathbf{q}}$) is a diagonal matrix in $R^{n\times n}$, and $\dot{\mathbf{q}}$ is vector of diagonal element. Then, the matrix $\mathbf{V}$ is obtained by inserting a *zero* value into diagonal positions for each column of $\mathbf{W}$.

3.3. *Minimum EEF velocity jump due to single locked joint faults*

If $\Delta\dot{\mathbf{x}} \neq 0$, then an EEF velocity jump has been occurred. By using Eq. (25) into Eq. (23), the minimum velocity jump of the EEF is indicated as

$$\Delta\dot{\mathbf{x}}_{\min} = -\mathbf{j}_k\dot{q}_k + {}^k\mathbf{J}{}^k\mathbf{u}^{\text{opt}}. \qquad (35)$$

Substituting ${}^k\mathbf{u}^{\text{opt}}$ that was obtained in Eq. (29) results in a velocity jump of

$$\Delta\dot{\mathbf{x}}_{\min} = -\mathbf{j}_k\dot{q}_k + {}^k\mathbf{J}({}^k\mathbf{J})^{\dagger}\mathbf{j}_k\dot{q}_k = ({}^k\mathbf{J}({}^k\mathbf{J})^{\dagger} - \mathbf{I})\mathbf{j}_k\dot{q}_k, \qquad (36)$$

where $\mathbf{I} \in R^{m\times m}$ is an identity matrix. The reduced Jacobian matrices are assumed full rank but it may become skinny especially when multiple failures occur.

If the reduced Jacobian matrix is a square full rank or fat full-rank matrix, then using the pseudoinverse gives ${}^k\mathbf{J}({}^k\mathbf{J})^{\dagger} = \mathbf{I}$, and consequently, the EEF velocity jump becomes zero

$$\Delta\dot{\mathbf{x}}_{\min} = ({}^k\mathbf{J}({}^k\mathbf{J})^{\dagger} - I)\mathbf{j}_k\dot{q}_k = 0. \qquad (37)$$

Therefore, the velocity jump in Eq. (37) is always zero for square full rank and fat full rank reduced matrices. But if ${}^k\mathbf{J}$ becomes skinny full-rank matrix (when $\mathbf{J}$ is square), then by using the left inverse definition of pseudoinverse (31), the velocity jump is obtained as

$$\Delta\dot{\mathbf{x}}_{\min} = ({}^k\mathbf{J}(({}^k\mathbf{J})^{\mathrm{T}}\,{}^k\mathbf{J})^{-1}({}^k\mathbf{J})^{\mathrm{T}} - \mathbf{I})\mathbf{j}_k\dot{q}_k. \qquad (38)$$

In summary, the minimum EEF velocity jump for SLRMs under the locked joint failure is

$$\Delta\dot{\mathbf{x}}_{\min} = \begin{cases} 0 & \text{when } {}^k\mathbf{J} \text{ is square or fat full rank matrix,} \\ ({}^k\mathbf{J}(({}^k\mathbf{J})^{\mathrm{T}}\,{}^k\mathbf{J})^{-1}({}^k\mathbf{J})^{\mathrm{T}} - \mathbf{I})\,\mathbf{j}_k\dot{q}_k & \text{when } {}^k\mathbf{J} \text{ is skinny and full rank matrix.} \end{cases} \qquad (39)$$

Equation (39) can be used to study the conditions of having a zero EEF velocity jump when a failure occurs to the kth joint. The zero EEF velocity jump is equivalent to fully fault tolerance. If it is not possible to have a zero EEF velocity jump then, because it is a minimum EEF velocity jump, we call it optimal fault tolerance.

3.4. *Conditions of a zero EEF velocity jump*

From Eq. (39), the conditions of a zero EEF velocity jump are summarized as following:

(1) If the reduced Jacobian matrix is a square full rank or a fat full-rank matrix.
(2) If $\dot{q}_k = 0$ when ${}^k\mathbf{J}$ is a skinny matrix.
(3) If ${}^k\mathbf{J}(({}^k\mathbf{J})^{\mathrm{T}}\,{}^k\mathbf{J})^{-1}({}^k\mathbf{J})^{\mathrm{T}} = \mathbf{I}$ when ${}^k\mathbf{J}$ is a skinny matrix.
(4) If $\mathbf{j}_k$ belongs to null space of ${}^k\mathbf{J}(({}^k\mathbf{J})^{\mathrm{T}}\,{}^k\mathbf{J})^{-1}({}^k\mathbf{J})^{\mathrm{T}} - \mathbf{I}$ when ${}^k\mathbf{J}$ is a skinny matrix.

The first condition is for the case that the reduced Jacobian matrix is a square full rank or fat full-rank matrix. It was clearly observed from Eq. (39) that this case results to a zero EEF velocity jump. The last three conditions are observed from $({}^k\mathbf{J}(({}^k\mathbf{J})^{\mathrm{T}}\,{}^k\mathbf{J})^{-1}({}^k\mathbf{J})^{\mathrm{T}} - \mathbf{I})\mathbf{j}_k\dot{q}_k$, which was for the case when ${}^k\mathbf{J}$ is a skinny matrix. These conditions are discussed in continue and it is shown that the third and fourth conditions in the aforementioned list are not physically possible.

The second condition happens when $\dot{q}_k = 0$. In this case, the velocity of the locked joint prior to the fault is zero. It is clear that the fault in the previously stopped joint does not provide any EEF velocity jump.

The third condition for having a zero velocity jump was when ${}^k\mathbf{J}(({}^k\mathbf{J})^{\mathrm{T}}\,{}^k\mathbf{J})^{-1}({}^k\mathbf{J})^{\mathrm{T}} = \mathbf{I}$, the following *Statement* is used to explain the third condition:

Statement 1: If $\mathbf{A}$ is an arbitrary skinny full-rank matrix, then $\mathbf{A}(\mathbf{A}^{\mathrm{T}}\mathbf{A})^{-1}\mathbf{A}^{\mathrm{T}}$ is called the optimal projection into the column space of $\mathbf{A}$. From matrix algebra, the $\mathbf{A}(\mathbf{A}^{\mathrm{T}}\mathbf{A})^{-1}\mathbf{A}^{\mathrm{T}}$ will be an identity matrix, if and only if, it is a square and full-rank matrix and it is in contradiction to the skinny form of $\mathbf{A}$.

To have a physical interpretation of Statement 1, we know that the column space of the Jacobian matrix is the velocity space of the EEF. Therefore, ${}^k\mathbf{J}(({}^k\mathbf{J})^{\mathrm{T}}\,{}^k\mathbf{J})^{-1}({}^k\mathbf{J})^{\mathrm{T}}$ maps the faulty joint contribution into the EEF velocity space of the faulty manipulator. This mapping is complete when the range space of ${}^k\mathbf{J}$ covers the velocity space, which is equivalent to the range space of $\mathbf{J}$. Therefore, the range space of ${}^k\mathbf{J}$ is required to be equal to the range space of $\mathbf{J}$. This implies that the column rank of matrix ${}^k\mathbf{J}$ has to be equal to the column rank of $\mathbf{J}$. Here is the contradiction because ${}^k\mathbf{J}$ is a skinny full rank and $\mathbf{J}$ is a square full-rank matrices and it is not possible to have the same column rank.

The fourth condition of a zero velocity jump is when $\mathbf{j}_k$ belongs to the null space ${}^k\mathbf{J}(({}^k\mathbf{J})^{\mathrm{T}}\,{}^k\mathbf{J})^{-1}({}^k\mathbf{J})^{\mathrm{T}} - \mathbf{I}$. The following *Statement* is used to explain this condition.

Statement 2: It is known that ${}^k\mathbf{J}(({}^k\mathbf{J})^{\mathrm{T}}\,{}^k\mathbf{J})^{-1}({}^k\mathbf{J})^{\mathrm{T}} - \mathbf{I}$ is the null space projection of ${}^k\mathbf{J}^{\mathrm{T}}$. It maps $\mathbf{j}_k\dot{q}_k$ into the null space of ${}^k\mathbf{J}^{\mathrm{T}}$. If $\mathbf{j}_k$ is in the null space of ${}^k\mathbf{J}(({}^k\mathbf{J})^{\mathrm{T}}\,{}^k\mathbf{J})^{-1}({}^k\mathbf{J})^{\mathrm{T}} - \mathbf{I}$, then it is in the row space of ${}^k\mathbf{J}^{\mathrm{T}}$. It clearly requires $\mathbf{j}_k$ to be a linear combination of the columns of ${}^k\mathbf{J}$. Consequently, the column rank of ${}^k\mathbf{J}$ needs to be the same as the column rank of $\mathbf{J}$ because $\mathbf{j}_k$ is linear combination of other columns of

https://doi.org/10.1017/S0263574711000671 Published online by Cambridge University Press

${}^{k}\mathbf{J}$. This is impossible because $\mathbf{J}$ is square full-rank matrix; therefore, the columns of $\mathbf{J}$ are independent.

From the list of four aforementioned conditions, it was understood that the only two following conditions are necessary and sufficient conditions for a zero EEF velocity jump:

(1) When the reduced Jacobian matrix is a full-rank square or full-rank fat matrix.
(2) When the velocity of the locked joint at failure time is zero.

4. Extension Toward Multiple Locked Joint Faults

4.1. Extension for two locked joint failures

The extension for two locked joint faults is obtained by using the perturbation methodology, which was indicated earlier for single joint failure. If the two locked joints are kth and lth joints of the manipulator (let say $k < l$), then the perturbation model for the velocity jump in Eq. (22) can be used when its parameter is defined according to these failures. Removing the columns of the Jacobian matrix due to the faults gives the Jacobian matrix perturbation as

$$\Delta\mathbf{J} = [0 \quad \dots \quad -\mathbf{j}_k \quad 0 \quad \dots \quad -\mathbf{j}_l \quad 0 \quad \dots \quad 0], \tag{40}$$

and if it is used in Eq. (22) then gives the EEF velocity jump as

$$\Delta\dot{\mathbf{x}} = -\mathbf{j}_k\dot{q}_k - \mathbf{j}_l\dot{q}_l + (\mathbf{J} + \Delta\mathbf{J})\mathbf{u}. \tag{41}$$

Similar to the expansion that was shown in Eq. (26), it is easy to show that

$$(\mathbf{J} + \Delta\mathbf{J})\mathbf{u} = {}^{k,l}\mathbf{J}^{k,l}\mathbf{u}. \tag{42}$$

Therefore, the EEF velocity jump is

$$\Delta\dot{\mathbf{x}} = -\mathbf{j}_k\dot{q}_k - \mathbf{j}_l\dot{q}_l + {}^{k,l}\mathbf{J}^{k,l}\mathbf{u}, \tag{43}$$

where ${}^{k,l}\mathbf{u}$ is the control input to minimize the EEF velocity jump due to the faults. Equation (43) is solved that gives the optimal control input for the fault tolerance of the manipulator as

$${}^{k,l}\mathbf{u}^{\text{opt}} = ({}^{k,l}\mathbf{J})^{\dagger}(\mathbf{j}_k\dot{q}_k + \mathbf{j}_l\dot{q}_l). \tag{44}$$

The pseudoinverse $({}^{k,l}\mathbf{J})^{\dagger}$ in Eq. (44) requires that the reduced Jacobian to be full rank.

Finally, the optimal input for compensating velocity jump of the EEF is

$$\mathbf{u}^{\text{opt}} = \left[{}^{k,l}u_1^{\text{opt}} \dots {}^{k,l}u_{k-1}^{\text{opt}} \; 0 \; {}^{k,l}u_k^{\text{opt}} \; \dots \; {}^{k,l}u_{l-1}^{\text{opt}} \; 0 \; {}^{k,l}u_l^{\text{opt}} \dots {}^{k,l}u_{n-2}^{\text{opt}}\right]^{\mathrm{T}}. \tag{45}$$

For determining the minimum velocity jump, if ${}^{k,l}\mathbf{J}$ is full-rank matrix, then the velocity jump for two locked joints failure is derived using Eq. (44) in Eq. (43) as

$$\Delta\dot{x}_{\min} = ({}^{k,l}\mathbf{J}({}^{k,l}\mathbf{J})^{\dagger} - \mathbf{I})(\mathbf{j}_k\dot{q}_k + \mathbf{j}_l\dot{q}_l). \tag{46}$$

If the reduced Jacobian matrix of ${}^{k,l}\mathbf{J}$ is fat full-rank matrix, then pseudoinverse is defined by the right inverse of ${}^{k,l}\mathbf{J}$ and for the right inverse we have ${}^{k,l}\mathbf{J}({}^{k,l}\mathbf{J})^{\dagger} = \mathbf{I}$, which results to a zero EEF velocity jump. When ${}^{k,l}\mathbf{J}$ is a square full-rank matrix, then ${}^{k,l}\mathbf{J}({}^{k,l}\mathbf{J})^{\dagger} = \mathbf{I}$ that results to a zero EEF velocity jump. But when ${}^{k,l}\mathbf{J}$ is a skinny full-rank matrix, then the left inverse of ${}^{k,l}\mathbf{J}$ is used and the EEF velocity jump is obtained by

$$\Delta\dot{\mathbf{x}}_{\min} = ({}^{k,l}\mathbf{J}(({}^{k,l}\mathbf{J})^{\mathrm{T}}\,{}^{k,l}\mathbf{J})^{-1}({}^{k,l}\mathbf{J})^{\mathrm{T}} - \mathbf{I})(\mathbf{j}_k\dot{q}_k + \mathbf{j}_l\dot{q}_l). \tag{47}$$

For a zero EEF velocity jump, in addition to the conditions that were mentioned for single joint failures, a new condition exists. This condition occurs if $\mathbf{j}_k\dot{q}_k$ and $\mathbf{j}_l\dot{q}_l$ do not independently belong to the null space of ${}^{k,l}\mathbf{J}(({}^{k,l}\mathbf{J})^{\mathrm{T}}\,{}^{k,l}\mathbf{J})^{-1}({}^{k,l}\mathbf{J})^{\mathrm{T}} - \mathbf{I}$, but their sum $\mathbf{j}_k\dot{q}_k + \mathbf{j}_l\dot{q}_l$ is in this null space. Physically, this can happen when the kth and the lth joints are canceling the contribution of each other. Therefore, their motion belongs to the self-motion manifold of the manipulator. In this case, if both joints fail at the same time, no EEF velocity jump occurs.

4.2. Extension for multiple faults: A general mapping

The extension toward multiple faults is proposed in this section. The extension can be derived by the perturbation method. The perturbations are required to be defined from the list of the faulty joints same as what was done for two faults. If $r \le n$ is the number of the locked joint faults, then the extension of the mapping framework for fault tolerance is derived as

$${}^{S_r}\mathbf{u}^{opt} = ({}^{S_r}\mathbf{J})^{\dagger}\left(\sum_{k\in S_r}\mathbf{j}_k\dot{q}_k\right) \tag{48}$$

for set of faulty joint S_r when $S_r = \{i_1\, i_2 \dots i_r |\; i_1 < i_2 < \dots < i_r;\ 1 \le i_1, i_2, \dots i_r \le n\}$, the optimal input is obtained analogically to that was indicated for fault tolerance of two joint failures in Eq. (44). S_r and ${}^{S_r}\mathbf{J}$ were previously introduced in Eq. (16). ${}^{S_r}\mathbf{J}$ was obtained by eliminating the columns of $\mathbf{J}$ associated to the faults determined by S_r. If ${}^{S_r}\mathbf{J}$ remains full rank then the pseudoinverse in Eq. (48) is meaningful and the EEF velocity jump of either for fat full rank, square full rank, or skinny full rank matrix of ${}^{S_r}\mathbf{J}$ gives $\Delta\dot{\mathbf{x}}_{\min} = ({}^{S_r}\mathbf{J}({}^{S_r}\mathbf{J})^{\dagger} - \mathbf{I})(\sum_{k\in S_r}\mathbf{j}_k\dot{q}_k)$.

When the reduced Jacobian matrix with multiple faults is still square full rank or fat full rank, then using the regular inverse or right inverse of ${}^{S_r}\mathbf{J}$ results in ${}^{S_r}\mathbf{J}({}^{S_r}\mathbf{J})^{\dagger} = \mathbf{I}$, which gives a zero EEF velocity jump. But if the reduced Jacobian matrix is skinny full-rank matrix, the velocity jump is obtained by the left inverse of ${}^{S_r}\mathbf{J}$ and it gives the EEF velocity jump as

$$\Delta\dot{\mathbf{x}}_{\min} = ({}^{S_r}\mathbf{J}(({}^{S_r}\mathbf{J})^{\mathrm{T}}\,{}^{S_r}\mathbf{J})^{-1}({}^{S_r}\mathbf{J})^{\mathrm{T}} - \mathbf{I})\left(\sum_{k\in S_r}\mathbf{j}_k\dot{q}_k\right). \tag{49}$$

The conditions of a zero EEF velocity jump include three conditions. The first is when the reduced Jacobian matrix remains square full rank or fat full-rank matrix, the second is when the velocity of the all locked joints at failure time is zero. The third is when the faulty joints motion was in the self-motion of the manipulator or $\sum_{k\in S_r}\mathbf{j}_k\dot{q}_k = 0$. Physically, this can happen when the faulty joints are canceling the contribution of each other to the velocity of the EEF. Hence, their motion belongs to the self-motion manifold of the manipulator, if all fail at the same time, no EEF velocity jump occurs.

4.3. *QR-decomposition and minimum velocity jump problem*

Motivated by the benefits of QR-decomposition and by knowing that in QR-decomposition, the matrix $\mathbf{Q}$ is an orthogonal matrix or $\mathbf{QQ}^{\mathrm{T}} = \mathbf{I}$, and $\mathbf{R}$ is an upper triangular matrix, one can simplify the results provided in Eqs. (48) and (49). The QR-decomposition for the Jacobian matrix is

$$\mathbf{J} = \mathbf{QR}. \tag{50}$$

If QR-decomposition for the reduced Jacobian matrix ${}^{S_r}\mathbf{J}$ is indicated by

$${}^{S_f}\mathbf{J} = \tilde{\mathbf{Q}}\tilde{\mathbf{R}}. \tag{51}$$

Then, $\tilde{\mathbf{Q}}$ is an orthogonal matrix or $\tilde{\mathbf{Q}}^{-1} = \tilde{\mathbf{Q}}^{\mathrm{T}}$. The optimum joint velocity control input in Eq. (48) is obtained as

$${}^{S_r}\mathbf{u}^{opt} = ({}^{S_r}\mathbf{J})^{\dagger}\left(\sum_{k\in S_r}\mathbf{j}_k\dot{q}_k\right) = \tilde{\mathbf{R}}^{\dagger}\tilde{\mathbf{Q}}^{\mathrm{T}}\left(\sum_{k\in S_r}\mathbf{j}_k\dot{q}_k\right), \tag{52}$$

and the EEF velocity jump is obtained as

$$\Delta\dot{\mathbf{x}}_{\min} = \tilde{\mathbf{Q}}(\tilde{\mathbf{R}}\tilde{\mathbf{R}}^{\dagger} - \mathbf{I})\tilde{\mathbf{Q}}^{\mathrm{T}}\left(\sum_{k\in S_r}\mathbf{j}_k\dot{q}_k\right). \tag{53}$$

This velocity jump is true either for case that the reduced Jacobian matrix remains square full rank, fat full rank, or skinny full-rank matrix. If the reduced Jacobian matrix is square full rank or fat full rank, then using the regular inverse or the right inverse of ${}^{S_r}\mathbf{J}$ gives $\tilde{\mathbf{R}}\tilde{\mathbf{R}}^{\dagger} = \mathbf{I}$, which results to a zero EEF velocity jump. But if the Jacobian matrix is a skinny full-rank matrix, then the left inverse of ${}^{S_r}\mathbf{J}$ is used and the EEF velocity jump is obtained by

$$\Delta\dot{\mathbf{x}}_{\min} = \tilde{\mathbf{Q}}(\tilde{\mathbf{R}}(\tilde{\mathbf{R}}^{\mathrm{T}}\tilde{\mathbf{R}})^{-1}\tilde{\mathbf{R}}^{\mathrm{T}} - \mathbf{I})\tilde{\mathbf{Q}}^{\mathrm{T}}\left(\sum_{k\in S_r}\mathbf{j}_k\dot{q}_k\right). \tag{54}$$

5. Generalized Optimal Mapping and Velocity Jump

This section summarizes the results of the previous sections. The framework for a generalized optimal mapping with a minimum EEF velocity jump is presented in a form of a theorem. Then, it outlines conditions of a zero EEF velocity jump.

5.1. *Generalized optimal mapping*

Theorem: The optimal mapping with a minimum EEF velocity jump is introduced as follows:

If $\mathbf{J} \in R^{m\times n}$ is the Jacobian matrix of a serial manipulator at a given nonsingular configuration, and if the manipulator is subjected to r locked joint failures ($r \le n$), and if the faults are indicated by an ascending set of

$$S_r = \{i_1\, i_2\, \ldots\, i_r \,|\, i_1 < i_2 < \ldots < i_r;\ \ 1 \le i_1, i_2, \ldots, i_r \le n\,\}. \tag{55}$$

Then, the optimum control input for the healthy joint ${}^{S_r}\mathbf{u}^{\mathrm{opt}}$ is obtained by

$${}^{S_r}\mathbf{u}^{\mathrm{opt}} = ({}^{S_r}\mathbf{J})^{\dagger}\left(\sum_{k\in S_r}\mathbf{j}_k\dot{q}_k\right), \tag{56}$$

where $({}^{S_r}\mathbf{J})^{\dagger}$ is the pseudoinverse of ${}^{S_r}\mathbf{J}$, and ${}^{S_r}\mathbf{J}$ is the reduced Jacobian matrix of $\mathbf{J}$. The pseudoinverse of a square full-rank matrix is the inverse of the matrix; for fat full-rank matrix, it is the right inverse of ${}^{S_r}\mathbf{J}$, which is $({}^{S_r}\mathbf{J})^{\dagger} = ({}^{S_r}\mathbf{J})^{\mathrm{T}}({}^{S_r}\mathbf{J}({}^{S_r}\mathbf{J})^{\mathrm{T}})^{-1}$. The pseudoinverse of the skinny full-rank matrix of ${}^{S_r}\mathbf{J}$ is the left inverse of ${}^{S_r}\mathbf{J}$, which is$({}^{S_r}\mathbf{J})^{\dagger} = (({}^{S_r}\mathbf{J})^{\mathrm{T}}\,{}^{S_r}\mathbf{J})^{-1}({}^{S_r}\mathbf{J})^{\mathrm{T}}$.

5.2. *Minimum EEF velocity jump*

If the mapping in Eq. (56) is used then the EEF velocity jump is a minimum EEF velocity jump. This minimum EEF velocity jump is calculated as

$$\Delta\dot{\mathbf{x}}_{\min} = ({}^{S_r}\mathbf{J}({}^{S_r}\mathbf{J})^{\dagger} - \mathbf{I})\left(\sum_{k\in S_r}\mathbf{j}_k\dot{q}_k\right). \tag{57}$$

For nonsingular configurations, ${}^{S_r}\mathbf{J}$ is a full rank. Depending to the size of ${}^{S_r}\mathbf{J}$ if regular, right or left inverse is used instead of pseudoinverse, then the minimum EEF velocity jump is

$$\Delta\dot{x}_{\min} = \begin{cases} 0, & \text{when } {}^{S_r}\mathbf{J} \text{ is square/fat full rank matrix,} \\ ({}^{S_r}\mathbf{J}(({}^{S_r}\mathbf{J})^{T}\,{}^{S_r}\mathbf{J})^{-1}({}^{S_r}\mathbf{J})^{T} - \mathbf{I})\left(\sum_{k\in S_r}\mathbf{j}_k\dot{q}_k\right), & \text{when } {}^{S_r}\mathbf{J} \text{ is skinny full rank matrix.} \end{cases} \tag{58}$$

5.3. *Conditions of a zero EEF velocity jump*

By using Eq. (58), a zero EEF velocity jump is achieved when the following conditions exist:

(1) If the reduced Jacobian matrix ${}^{S_r}\mathbf{J}$ faults square full rank or fat full-rank matrix.
(2) If velocities of the faulty joints at to fault time are zero when ${}^{S_r}\mathbf{J}$ is a skinny full rank.
(3) If $\sum_{k\in S_r}\mathbf{j}_k\dot{q}_k = 0$, the faulty joint velocities are not zero and ${}^{S_r}\mathbf{J}$ is skinny full rank.

To demonstrate the validity of this generalized framework, three case studies are implemented in the following sections.

6. Case Study I: Optimal Mapping for a 5-DOF Planar Manipulator

A 5-DOF planar manipulator is modeled using MATLAB Robotics Toolbox.[38] The Denavit–Hartenberg (D-H)

https://doi.org/10.1017/S0263574711000671 Published online by Cambridge University Press

Table I. D-H parameters of a 5-DOF planar manipulator.

Link	s_k (m)	d_k (m)	α_k	q_k
1	0.05	0.45	0	q_1
2	0.05	0.32	0	q_2
3	0.05	0.18	0	q_3
4	0.05	0.12	0	q_4
5	0.05	0.08	0	q_5

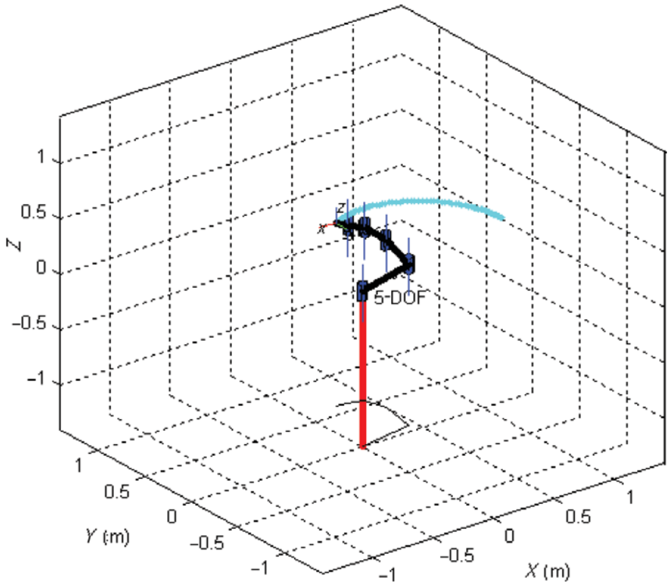

Fig. 1. (Colour online) A 5-DOF planar manipulator and sample of planar trajectory, the reference frame for the Jacobian matrices is in the frame attached to the EEF.

parameters of the manipulator are shown in Table I. In D-H parameters, s_k is the joint offset, q_k is the joint angle, d_k is the link length, and α_k is the link twist angle. The manipulator's configuration parameters and the joint velocities at the configuration shown in Fig. 1 are indicated in Table II. For this configuration and the indicated joint velocities, the velocity of the EEF of the manipulator is $\dot{\mathbf{x}} = [0.26\ 0.20]^T$ m/s.

The last column of Table II is computed by $\|\mathbf{j}_k\dot{q}_k\|/\|\dot{\mathbf{x}}\|$, which indicates how much each joint contributes to the motion of the manipulator and it is divided by the velocity of the EEF.

Four fault scenarios have been tested by using the model of the manipulator. The fault scenarios include some cases of a single failure up to four locked joint failures.

6.1. Scenario 1: Single joint faults

There are five cases of single joint failures. All five cases are considered in scenario 1. The positional Jacobian matrix of the manipulator in the reference frame attached to the EEF of the manipulator is obtained as

$$\mathbf{J} = \begin{bmatrix} 0.64 & 0.48 & 0.16 & 0.00 & 0.00 \\ -0.15 & 0.27 & 0.27 & 0.20 & 0.08 \end{bmatrix}. \tag{59}$$

In the first case of single joint failures, if the first joint fails, then the reduced Jacobian matrix and the eliminated column of $\mathbf{J}$ are

$$^{1}\mathbf{J} = \begin{bmatrix} 0.48 & 0.16 & 0.00 & 0.00 \\ 0.27 & 0.27 & 0.20 & 0.08 \end{bmatrix}, \tag{60}$$

$$\mathbf{j}_1 = \begin{bmatrix} 0.64 \\ -0.15 \end{bmatrix}. \tag{61}$$

The optimal control input to tolerate the first joint failure is obtained via the mapping (29) as

$$^{1}\mathbf{u}^{\text{opt}} = (^{1}\mathbf{J})^{\dagger}\mathbf{j}_1\dot{q}_1 \Rightarrow {}^{1}\mathbf{u}^{\text{opt}} = [\,0.08\ -0.04\ -0.08\ -0.03\,]^{T}\text{rad/s}, \tag{62}$$

which is a required change of the velocity for second, third, fourth, and fifth joints to compensate the first joint fault. By Eq. (32), $\mathbf{u}^{\text{opt}} = [0\ \ 0.08\ \ -0.04\ \ -0.08\ \ -0.03\,]^T$. Then, the vector of joint velocities is $\dot{\mathbf{q}} = [0\ \ 0.48\ \ 0.16\ \ 0.02\ \ 0.27\,]$ rad/s that maintains the EEF velocity. The next step is to calculate the EEF velocity jump. The EEF velocity jump is determined via $\Delta\dot{\mathbf{x}}_{\min} = (^{1}\mathbf{J}(^{1}\mathbf{J})^{\dagger} - \mathbf{I})\mathbf{j}_1\dot{q}_1$. Substitution of the parameters results in a zero EEF velocity jump. Zero jump is confirmed if $\dot{\mathbf{q}} = [0\ \ 0.48\ \ 0.16\ \ 0.02\ \ 0.27\,]$ rad/s is used with the Jacobian matrix of the healthy manipulator, which indicates fully fault tolerance.

The same approach as the one for the fault in first joint is used for other single joint failures. Table III presents joint velocities for the fault tolerance of any of single joint faults. From the EEF velocity jump shown in the last row of the table, the fully faults tolerance is observed for all single joint failures.

Table II. Joint velocities and joint angels of the planar manipulator at a fault instance. These are used in all fault scenarios 1–4.

Joint No	Angle q in degree	Velocity $\dot{q}$ in rad/s	Contribution into the motion of the manipulator
1	10	0.05	0.10
2	70	0.40	0.67
3	25	0.20	0.20
4	65	0.10	0.07
5	0	0.30	0.07

Table III. Joint velocities with minimum EEF velocity jump (values are in rad/s).

Joint No.	Second joint fault	Third joint fault	Fourth joint fault	Fifth joint fault
1	0.26	0.01	0.02	0.02
2	0	0.52	0.43	0.43
3	0.56	0	0.23	0.23
4	0.29	0.18	0	0.12
5	0.38	0.33	0.31	0
Velocity Jump	0.00 m/s	0.00 m/s	0.00 m/s	0.00 m/s

https://doi.org/10.1017/S0263574711000671 Published online by Cambridge University Press

Table IV. Joint velocities with minimum EEF velocity jump (values are in rad/s).

Joint No.	Second and third joint fault	Second and fourth joint fault
1	0.40	0.22
2	0	0
3	0	0.73
4	1.04	0
5	0.68	0.42
Velocity jump	0.00 m/s	0.00 m/s

Table V. Joint velocities with minimum EEF velocity jump (values are in rad/s).

Joint No.	Second, third, and fourth joint fault	Second, fourth, and fifth joint fault
1	0.40	0.19
2	0	0
3	0	0.83
4	0	0
5	3.27	0
Velocity jump	0.00m/s	0.00m/s

Table VI. D-H parameters of a 5-DOF spatial manipulator.

Link	s_k (m)	d_k (m)	α_k (Deg)	q_k
1	0.05	0.45	0	q_1
2	0.05	0.32	90	q_2
3	0.05	0.18	0	q_3
4	0.05	0.12	0	q_4
5	0.05	0.08	0	q_5

6.2. Scenario 2: Two joint faults

There are ten cases of two joint failures. Two of the cases including the faults in second and third joints and the faults in second and fourth joints are studied in this scenario. The Jacobian matrix in Eq. (59) is used to obtain under the mapping in Eq. (44) and the results of the optimal mapping are shown in Table IV. The minimum velocity jump is obtained by Eq. (45).

6.3. Scenario 3: Three joint faults

There are ten cases of three joint failures. In this scenario, two of these ten cases including the faults of second, third, and fourth joints and the faults of second, fourth, and fifth joints are studied. The Jacobian matrix in Eq. (59) is used with the framework in Eqs. (56) and (57). Table V shows the results of the optimal mapping and the EEF minimum velocity jumps.

6.4. Scenario 4: Four joint faults

There are five cases of four joint failures. In this scenario, the one with the fault in the second, third, fourth, and fifth joints is studied. The Jacobian matrix in Eq. (59) is used under the framework in Eqs. (56) and (57) and optimal joint velocity is then computed as $\dot{\mathbf{q}} = [0.31 \quad 0 \quad 0 \quad 0 \quad 0]^{\mathrm{T}}$ rad/s. The minimum EEF velocity jump is then obtained as $\Delta\dot{\mathbf{x}}_{\min} = [-0.06 \quad -0.25]^{\mathrm{T}}$ m/s. The norm of the velocity jump is $\|\Delta\dot{\mathbf{x}}_{\min}\| = 0.26$ m/s.

Table VII. Joint velocities and joint angels of the manipulator at fault instance. These are used in all fault scenarios 1–4.

Joint No.	Angle q (deg)	Velocity $\dot{q}$ (rad/s)	Contribution into motion of the manipulator
1	10	0.05	0.19
2	70	0.40	0.89
3	25	0.20	0.28
4	65	0.10	0.09
5	0	0.30	0.11

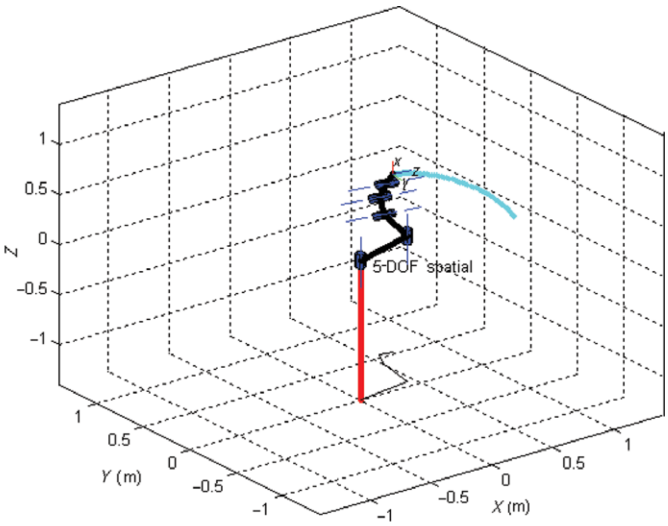

Fig. 2. (Colour online) A 5-DOF spatial manipulator, the reference frame for the Jacobian matrices is in the frame attached to the EEF.

The above scenarios indicate that the faults up to three joints are fully compensated because the manipulator has 5-DOF and the workspace is R^2. But in the fourth scenario with one healthy joint, the framework does not fully compensate the EEF velocity jump. However, the provided joint velocities result in a minimum EEF velocity jump. These observations are consistent with the conditions of a zero velocity jump. It was mentioned earlier that the reference frame of the Jacobian matrix is the frame attached to the EEF. Similar EEF velocity jump is observed if the Jacobian matrix is calculated in the reference frame attached to the base of the manipulator.

7. Case Study II: Optimal Mapping for a Spatial 5-DOF Manipulator

A 5-DOF manipulator with the D-H parameters shown in Table VI is modeled using MATLAB Robotic Toolbox. The aim of this case study is to investigate the framework in Eqs. (57) and (58) for maintaining the linear velocity of the EEF of nonplanar manipulator. Table VII indicates the joint angles and joint velocities of the manipulator. These parameters have been used for the four fault scenarios in this section. The configuration of the manipulator in Table VII is indicated in Fig. 2. The EEF velocity at this configuration is $\Delta\dot{\mathbf{x}}_{\min} = [0.03 \quad 0.01 \quad -0.22]^{\mathrm{T}}$ m/s.

https://doi.org/10.1017/S0263574711000671 Published online by Cambridge University Press

Table VIII. Joint velocities with minimum EEF velocity jump (values are in rad/s).

Joint No.	Second joint fault	Third joint fault	Fourth joint fault	Fifth joint fault
1	0.35	−0.03	0.03	0.01
2	0	0.50	0.46	0.45
3	0.20	0	0.20	0.20
4	0.59	0.21	0	0.15
5	0.50	0.34	0.33	0
Velocity jump	0.00 m/s	0.03 m/s	0.00 m/s	0.00 m/s

The framework for single joint failure in Eq. (29), two joint failures in Eq. (44), three and four joint failures in Eq. (56) are examined with four fault scenarios in below.

The manipulator positional Jacobian matrix in the reference frame attached to the EEF is

$$\mathbf{J} = \begin{bmatrix} 0.00 & 0.00 & 0.16 & 0.00 & 0.00 \\ -0.57 & -0.15 & 0.28 & 0.20 & 0.08 \\ -0.64 & -0.48 & 0.00 & 0.00 & 0.00 \end{bmatrix}. \quad (63)$$

7.1. Scenario 1: Single joint failure

There are five cases of single joint failures. All five are considered in this scenario.

If the first joint fails, then the reduced Jacobian matrix and the eliminated column are

$$^{1}\mathbf{J} = \begin{bmatrix} 0.00 & 0.16 & 0.00 & 0.00 \\ -0.15 & 0.28 & 0.20 & 0.08 \\ -0.48 & 0.00 & 0.00 & 0.00 \end{bmatrix}, \quad (64)$$

$$\mathbf{j}_1 = [\,-0.00\ -0.57\ -0.64\,]^{\mathrm{T}}. \quad (65)$$

The control input for compensating the EEF velocity jump is obtained by $^{1}\mathbf{u}^{\mathrm{opt}} = (^{1}\mathbf{J})^{\dagger}\mathbf{j}_1\dot{q}_1$ as $^{1}\mathbf{u}^{\mathrm{opt}} = [0.07 \quad 0.00 \quad -0.08 \quad -0.03\,]^{\mathrm{T}}$ rad/s. This gives the optimal control input of $\mathbf{u}^{\mathrm{opt}}$ as $\mathbf{u}^{\mathrm{opt}} = [0.00 \quad 0.07 \quad 0.00 \quad -0.08 \quad -0.03\,]^{\mathrm{T}}$ rad/s. The optimal joint velocity with minimum EEF velocity jump is $\dot{\mathbf{q}} = [0.00 \quad 0.47 \quad 0.20 \quad 0.02 \quad 0.27\,]^{\mathrm{T}}$ rad/s. The velocity jump is determined by $\Delta\dot{\mathbf{x}}_{\mathrm{min}} = (^{1}\mathbf{J}(^{1}\mathbf{J})^{\dagger} - \mathbf{I})\mathbf{j}_1\dot{q}_1$. By substituting the values, the minimum EEF velocity jump is $\|\Delta\dot{\mathbf{x}}_{\mathrm{min}}\| = 0$ m/s. The zero EEF velocity jump is obtained because the reduced Jacobian matrix is full column rank. Table VIII indicates joint velocities for the failure of the other single joints. The joint velocities in each column of the tables have been calculated by the same approach as that for the first joint. The minimum EEF velocity jump is shown in the last row of the table. From the EEF velocity jump, it is observed that only the fault in the third joint causes a nonzero EEF velocity jump. The third joint is critical because losing this joint makes the reduced Jacobian matrix close to be rank deficient Jacobian matrix. For this failure, the minimum velocity jump is 0.03 m/s. The velocity jump vector is $\Delta\dot{\mathbf{x}}_{\mathrm{min}} = [-0.03 \quad 0 \quad 0\,]^{\mathrm{T}}$ m/s.

7.2. Scenario 2: Two joint faults

There are ten cases of two joint failures. Two of these cases are studied in this scenario. The results of the mapping are shown in Table IX. The second column of the table presents the optimal joint velocities when a fault occurs to second and third joints of the manipulator. For this case, the minimum velocity jump is 0.03 m/s and the EEF velocity jump vector is $\Delta\dot{\mathbf{x}}_{\mathrm{min}} = [-0.03 \quad 0 \quad 0\,]^{\mathrm{T}}$ m/s. The third column of the table is for the faults of second and fourth joints. In this case, fully fault tolerance has been achieved.

Table IX. Joint velocities with minimum EEF velocity jump (values are in rad/s).

Joint No.	Second and third joint fault	Second and fourth joint fault
1	0.35	0.35
2	0	0
3	0	0.20
4	0.83	0
5	0.59	1.97
Velocity jump	0.03 m/s	0.00 m/s

Table X. Joint velocities with minimum EEF velocity jump (values are in rad/s).

Joint No.	Second, third and fourth joint fault	Second, fourth and fifth joint fault
1	0.35	0.31
2	0	0
3	0	0.55
4	0	0
5	2.66	0
Velocity jump	0.03 m/s	0.07 m/s

7.3. Scenario 3: Three joint faults

There are ten cases of three joint failures. Two of these cases are studied in this scenario. The first one is for the fault in second, third, and fourth joints of the manipulator. The result of this case is shown in the second column in Table X. The minimum velocity jump is then 0.03 m/s. The EEF velocity jump vector is $\Delta\dot{\mathbf{x}}_{\mathrm{min}} = [-0.03 \quad 0 \quad 0\,]^{\mathrm{T}}$ m/s.

The second case is for the fault in second, fourth, and fifth joints. Results of the mapping for this case are shown in the third column of the table and the EEF velocity jump is 0.07 m/s. In this case, the EEF velocity jump vector is $\Delta\dot{\mathbf{x}}_{\mathrm{min}} = [0.06 \quad -0.03 \quad 0.03\,]^{\mathrm{T}}$m/s. The EEF velocity jump has been occurred because the reduced matrix is rank deficient.

7.4. Scenario 4: Four joint faults

There are five cases of four joint failures. In this scenario, the case where the fault occurs in *second*, *third*, *fourth*, and *fifth*

https://doi.org/10.1017/S0263574711000671 Published online by Cambridge University Press

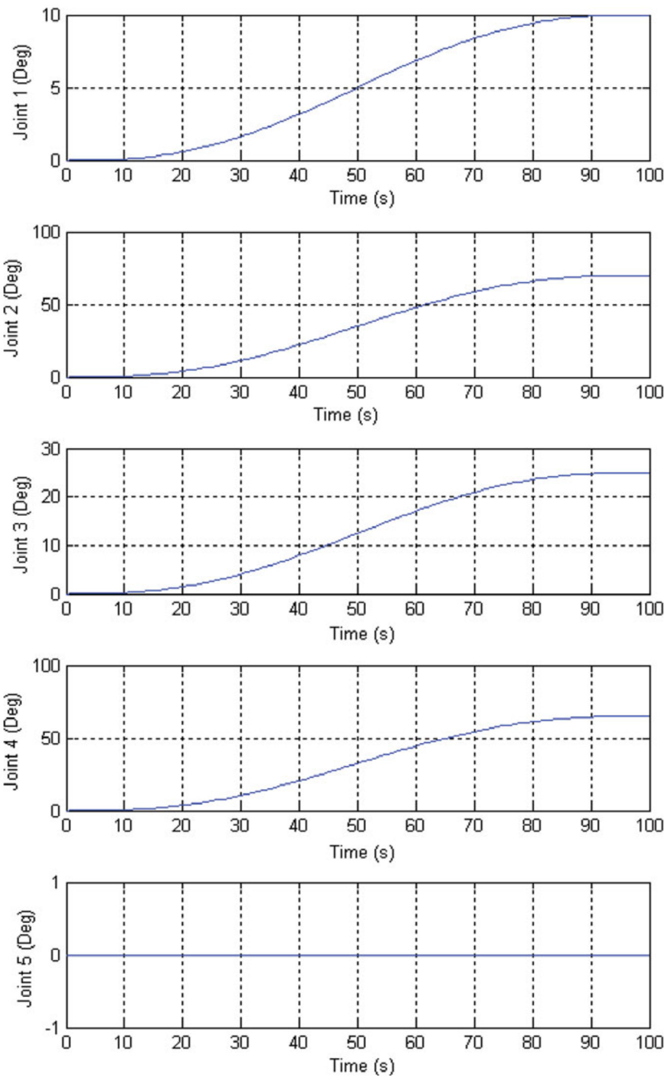

Fig. 3. (Colour online) Joint trajectories for the indicated trajectory in Fig.2. These trajectories are based on a trajectory design function in Matlab Robotics Toolbox.

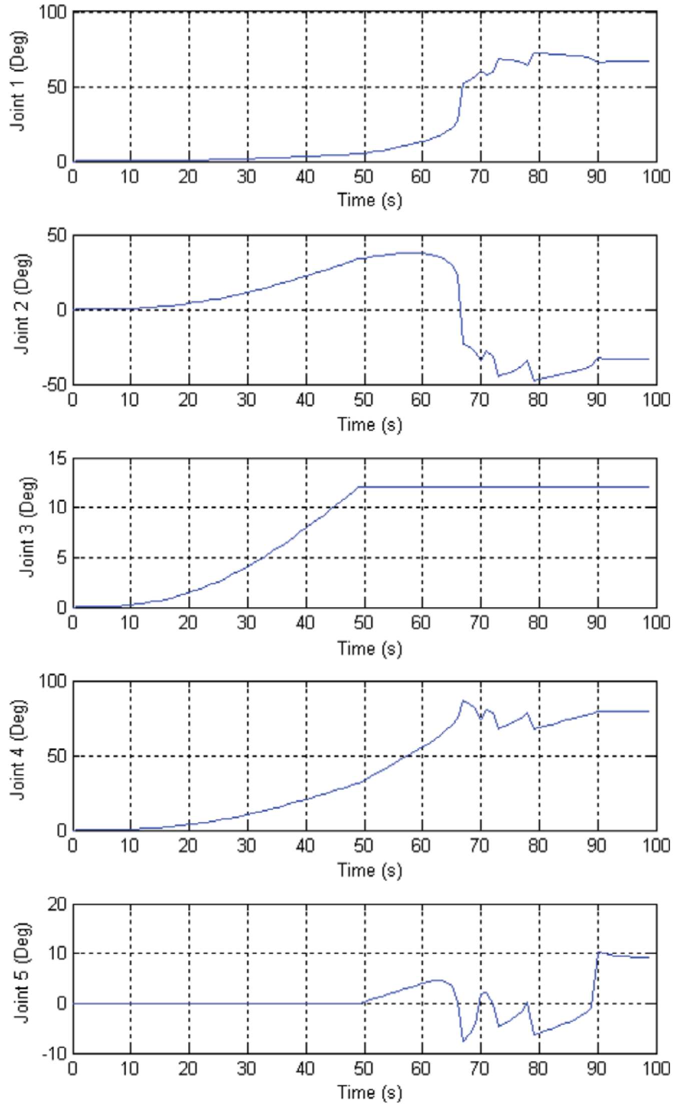

Fig. 4. (Colour online) Faulty manipulator's joint trajectory (the third joint locked at 50th second).

joints is studied. Using the generalized framework (56) and the Jacobian matrix in Eq. (63), the optimal joint velocity is obtained as $\dot{q} = [0.31 \quad 0 \quad 0 \quad 0 \quad 0]^{\mathrm{T}}$ rad/s. This joint velocity results to the minimum EEF velocity jump vector of $\Delta\dot{x}_{\min} = [0.06 \quad -0.03 \quad 0.03]^{\mathrm{T}}$ m/s. The norm of the minimum EEF velocity jump is $\|\Delta\dot{x}_{\min}\| = 0.073$ m/s.

8. Case Study III: A Simulation Study

The framework in Eqs. (56) and (57) can be used for whole workspace trajectory of the manipulator to optimally maintain the velocity of the EEF when it is subjected to a joint fault. The fault-tolerant operation of a 5-DOF positional manipulator with D-H parameters in Table VI is presented in this section. The workspace trajectory of the manipulator starts from $\mathbf{x}_s = [1.150 \quad -0.134 \quad 0.034]^{\mathrm{T}}$ m and ends to $\mathbf{x}_d = [0.781 \quad 0.509 \quad 0.280]^{\mathrm{T}}$ m. This trajectory is shown in Fig. 2. The corresponding joint trajectories are shown in Fig. 3.

Two simulations have been developed to move the EEF on the trajectory shown in Fig. 2. The first simulation is for the case of a healthy manipulator, and the second one is when the third joint of the manipulator is locked. The manipulator with the fault in the third joint is called faulty manipulator. The objective of the simulation is to find the manipulator's joint velocity and EEF trajectory for the healthy manipulator and the faulty manipulator. The proposed mapping is for the faulty manipulator used to maintain the EEF velocity of the healthy manipulator. The fault occurs at the 50th second of the motion to the faulty manipulator. A hundred seconds of the motion of both manipulators is implemented in these simulations. The third joint of the manipulator in the second simulation is locked at the 50th second. The required joint velocity commands to compensate this fault were computed and it is indicated in Fig. 4.

Seven snapshots of the motion of the healthy and faulty manipulator's have been captured and are shown in Fig. 5. They indicate the configurations of the healthy and faulty manipulators and their EEF trajectory. It is seen that even the trajectory has been efficiently maintained despite of the third joint failure. The first column of previous page is with the snapshots of the healthy manipulator, and the second

https://doi.org/10.1017/S0263574711000671 Published online by Cambridge University Press

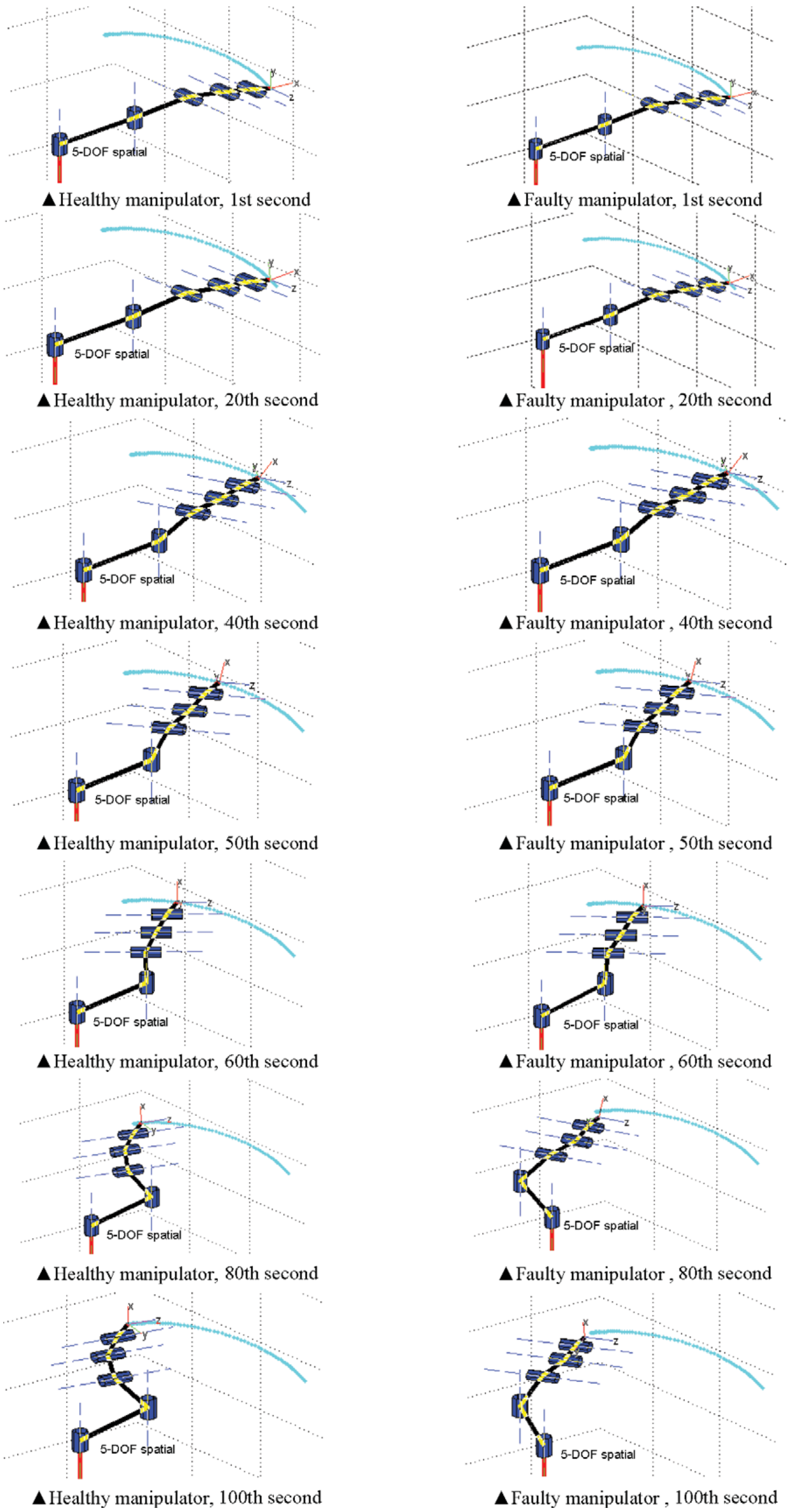

Fig. 5. (Colour online) Manipulators' configurations for indicated times. The first simulation results in left side are for the healthy manipulator and second simulation results in right side are for the faulty manipulator.

https://doi.org/10.1017/S0263574711000671 Published online by Cambridge University Press

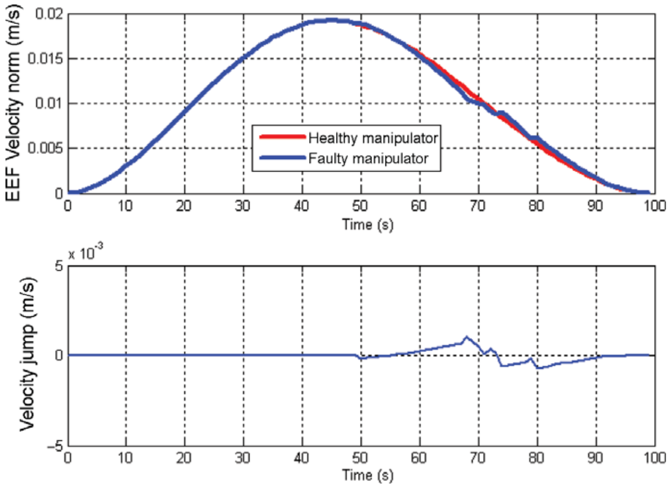

Fig. 6. (Colour online) EEF velocity for the healthy and the faulty manipulators and minimum EEF velocity jump.

column is with the corresponding snapshots for the faulty manipulator.

9. Discussion on the Case Studies

Results of the first two case studies for planar and positional manipulators confirm that the proposed framework and the conditions for having a zero velocity jump can be used for the fault tolerance of the robotic manipulators. For the case study III, we have extended the proposed framework for the whole motion of the manipulators. From the results of the simulations, the joint angle trajectories in Figs. 3 and 4 are exactly the same between 0 to 50th second. At the 50th second, the third joint is locked and it remains unchanged as Fig. 4 shows. After the failure time, the mapping framework is used maintain the EEF velocity.

Figure 6 compares the velocity of the EEF for the healthy manipulator and the faulty manipulator. The performance of compensation is good until the 65th second of the motion. At this time, the reduced Jacobian matrix is very close to be rank deficient and caused an indicated velocity jump. From the EEF velocity jump shown in Fig. 6, the maximum EEF velocity jump is determined as 0.0015 $m/$s. From the result of the figures in Table XI, the faulty manipulator has tried to maintain the trajectory of the healthy manipulator. This has been achieved by deploying the control input computed by via the proposed mapping in this paper.

9.1. Comparison of the proposed approach with other work on velocity jump

The minimum EEF velocity jump was studied in this paper. From the literature, there are a number of references, which have addressed the velocity jump. However, they have not covered all the aspects and the generalization that we have addressed in the present paper. For instance, a minimum JVJ for redundant manipulators has been addressed extensively in refs. [31, 32, 39, 40]. Within those work, the minimum JVJ has been achieved via a minimization problem subjected to a fault in kth joint. Following minimization problem has been used to achieve minimum JVJ:

$$\text{Min} \quad \frac{1}{2}({}^k\dot{\mathbf{q}} - \dot{\mathbf{q}})^{\mathrm{T}}({}^k\dot{\mathbf{q}} - \dot{\mathbf{q}}). \tag{66}$$

$$\text{Subjected to} \quad \dot{\mathbf{x}} = {}^k\mathbf{J}\,{}^k\dot{\mathbf{q}}, \tag{67}$$

where $\dot{\mathbf{q}}$ is the joint velocity vector prior the failure and ${}^k\dot{\mathbf{q}}$ is the joint velocity vector after the failure occurs. This minimization problem has been solved using Lagrange multiplier method and the optimal mapping with the minimum JVJ was derived:[31,32]

$${}^k\dot{\mathbf{q}} = ({}^k\mathbf{J})^{\dagger}\dot{\mathbf{x}}. \tag{68}$$

It is clear, that the work in refs. [31, 32] is not addressing the minimum EEF velocity jump; however, they are assuming it zero. We have obtained an optimal mapping that can map the lost contribution of the faulty joint to the compensating joint velocities of the healthy joints instead of just reconfiguring the joint velocities. In the present work and by using matrix perturbation methodology, a generalized framework is proposed. This framework includes the cases with either single or multiple joint failures.

10. Conclusion

Optimal fault mapping was presented in this paper to tolerate the effect of the locked joint failures on the EEF velocity of SLMs. The perturbation methodology was used for the study of the locked joint failures of the manipulators to obtain the EEF velocity jump due to the failures. Then, via least-square technique, the minimum EEF velocity jump was obtained through a mapping. The concepts and mathematical properties of the proposed mapping were discussed. Extension of the mapping for multiple locked joint failures was presented and a general framework for the mapping was introduced. The mapping gives the control law to minimize the EEF velocity jump when locked joint faults occur to the manipulators. The conditions for a zero EEF velocity jump were addressed.

The proposed mapping framework was evaluated for optimal fault tolerance of the positional velocities of a planar manipulator and a spatial manipulator in three case studies. The first two case studies validated the proposed mapping for instantaneous fault tolerance by calculating the velocity jumps for different fault scenarios in a given configuration of manipulators. The third case study used the proposed framework for a faulty manipulator to optimally maintain the EEF velocity and EEF trajectory provided by a healthy manipulator.

Acknowledgments

This research was supported by Centre for Intelligent Systems Research, Deakin University, Australia and in part by the US National Science Foundation under Contract IIS-0812437. The authors would also like to thank anonymous reviewers and Dr. Zoran Najdovski for their constructive comments, which greatly improved this paper.

References

1. E. Wu, M. Diftler, J. Hwang and J. Chladek, "A Fault Tolerant Joint Drive System for the Space Shuttle Remote Manipulator System," *Proceedings of the IEEE International Conference on Robotics and Automation*, Sacramento, CA, USA (1991) pp. 2504–2509.
2. M. Goel, A. A. Maciejewski, V. Balakrishnan and R. W. Proctor, "Failure tolerant teleoperation of a kinematically redundant manipulator: An experimental study," *IEEE Trans. Syst. Man Cyber. Part A: Syst. Humans* **33**, 758–765 (2003).
3. B. M. Harpel, J. B. Dugan, I. D. Walker and J. R. Cavallaro, "Analysis of Robots for Hazardous Environments," *Proceedings of the Annual Reliability and Maintainability Symposium*, Philadelphia, PA, USA (1997) pp. 111–116.
4. R. Colbaugh and M. Jamshidi, "Robot manipulator control for hazardous waste-handling applications," *J. Robot. Syst.* **9**, 215–250 (2007).
5. B. S. Dhillon, A. R. M. Fashandi and K. L. Liu, "Robot systems reliability and safety: A review," *J. Qual. Maint. Eng.* **8** (2002).
6. H. Abdi and S. Nahavandi, "Optimal Actuator Fault Tolerance for Static Nonlinear Systems Based on Minimum Output Velocity Jump," **In**: *IEEE International Conference on Information and Automation*, China, (2010) pp. 1165–1170.
7. Y. Yi, J. E. McInroy and F Jafari, "Optimum Design of a Class of Fault Tolerant Isotropic Gough-Stewart Platforms," *Proceedings of the IEEE International Conference on Robotics and Automation* (2004) pp. 4963–4968.
8. S. Tosunoglu and V. Monteverde, "Kinematic and structural design assessment of fault-tolerant manipulators," *Intell. Autom. Soft Comput.* **4**, 261–268 (1998).
9. L. Notash and L. Huang, "On the design of fault tolerant parallel manipulators," *Mech. Mach. Theory* **38**, 85–101 (2003).
10. J. E. McInroy, J. F. O'Brien and G. W. Neat, "Precise, fault-tolerant pointing using a Stewart platform," *IEEE/ASME Trans. Mechatronics* **4**, 91–95 (1999).
11. A. A. Maciejewski, "Fault Tolerant Properties of Kinematically Redundant Manipulators," *Proceedings of the IEEE International Conference on Robotics and Automation*, Cincinnati, OH, USA (1990) pp. 638–642.
12. H. Abdi and S. Nahavandi, "Designing Optimal Fault Tolerant Jacobian for Robotic Manipulators," *Proceedings of the IEEE/ASME International Conference on Advanced Intelligent Mechatronics*, Montréal, Canada (2010) pp. 426–431.
13. C. J. J. Paredis and P. K. Khosla, "Designing fault-tolerant manipulators: How many degrees of freedom?," *Int. J. Robot. Res.* **15**, 611–628 (1996).
14. R. G. Roberts, S. A. Siddiqui and A. A. Maciejewski, "Designing Equally Fault-Tolerant Configurations for Kinematically Redundant Manipulators," *Proceedings of the IEEE International Symposium on Sustainable Systems and Technology*, Tullahoma, TN, USA (2009) pp. 335–339.
15. R. G. Roberts, "On the local fault tolerance of a kinematically redundant manipulator," *J. Robot. Syst.* **13**, 649–661 (1998).
16. R. G. Roberts, "The dexterity and singularities of an underactuated robot," *J. Robot. Syst.* **18**, 159–169 (2001).
17. H. Abdi and S. Nahavandi, "Minimum Reconfiguration for Fault Tolerant Manipulators," *Proceedings of the 34th Annual Mechanisms and Robotics Conference, Parts A and B, ASME International Design Engineering Technical Conferences and Computers and Information in Engineering Conference (IDETC/CIE)*, Montreal, Quebec, Canada (2010), pp. 1345–1350.
18. F. Caccavale, P. Chiacchio and I. D. Walker, "A time-delayed observer for fault detection and isolation in industrial robots," *Robotica* **24**, 557–565 (2006).
19. C. Carreras and I. D. Walker, "Interval methods for fault-tree analysis in robotics," *IEEE Trans. Reliab.* **50**, 3–11 (2001).
20. L. Notash, "Joint sensor fault detection for fault tolerant parallel manipulators," *J. Robot. Syst.* **17**, 149–157 (2000).
21. J. Park, W. K. Chung and Y. Youm, "Failure Recovery by Exploiting Kinematic Redundancy," *Proceedings of the IEEE International Workshop on Robot and Human Communication* (1996) pp. 298–305.
22. J. M. Yang, "Fault-tolerant crab gaits and turning gaits for a hexapod robot," *Robotica* **24**, 269–270 (2006).
23. J. M. Yang, "Gait synthesis for hexapod robots with a locked joint failure," *Robotica* **23**, 701–708 (2005).
24. C. J. J. Paredis and P. K. Khosla, "Fault tolerant task execution through global trajectory planning," *Reliab. Eng. Syst. Saf.* **53**, 225–235 (1996).
25. Y. Chen, J. E. McInroy and Y. Yi, "Optimal, fault-tolerant mappings to achieve secondary goals without compromising primary performance," *IEEE Trans. Robot. Autom.* **19**, 680–691 (2003).
26. R. G. Roberts, "The dexterity and singularities of an underactuated robot," *J. Robot. Syst.* **18**, 159–169 (2001).
27. P. J. From and J. T. Gravdahl, "On the mobility and fault tolerance of closed chain manipulators with passive joints," *Model. Identif. Control* **29**, 151–165 (2008).
28. H. Abdi and S. Nahavandi, "Joint Velocity Redistribution for Fault Tolerant Manipulators," *Proceedings of the IEEE Conference on Robotics Automation and Mechatronics* (2010) pp. 492–497.
29. R. G. Roberts, H. G. Yu and A. A. Maciejewski, "Fundamental limitations on designing optimally fault-tolerant redundant manipulators," *IEEE Trans. Robot.* **24**, 1224–1237 (2008).
30. M. Güdemann, F. Ortmeier and W. Reif, "Formal Modeling and Verification of Systems with Self-x Properties," *Autonomic and Trusted Computing*, **4158**, 38–47 (2006).
31. J. Zhao, K. L. Zhang and D. D. Feng, "Sudden change of joint velocity during fault tolerant operations for redundant manipulators: Not available online," *Beijing Gongye Daxue Xuebao/J. Beijing Univ. Technol.* **33**, 1121–1125 (2007).
32. J. Zhao, Y. Yao and X. Yao, "On the Sudden Change in Joint Velocity during Fault Tolerant Operations for Spatial Coordinating Redundant Manipulators," *Proceedings of the IEEE International Conference on Intelligent Robots and Systems*, Beijing (2006) pp. 3885–3890.
33. R. G. Roberts, H. G. Yu and A. A. Maciejewski, "Fundamental limitations on designing optimally fault-tolerant redundant manipulators," *IEEE Trans. Robot.* **24**, 1224–1237 (2008).
34. C. L. Lewis and A. A. Maciejewski, "Fault tolerant operation of kinematically redundant manipulatorsfor locked joint failures," *IEEE Trans. Robot. Autom.* **13**, 622–629 (1997).
35. J. W. Burdick, "On the Inverse Kinematics of Redundant Manipulators: Characterization of the Self-Motion Manifolds," *Proceedings of the IEEE International Conference on Robotics and Automation* (1989) pp. 264–270.
36. R. G. Roberts and A. A. Maciejewski, "A local measure of fault tolerance for kinematically redundant manipulators," *IEEE Trans. Robot. Autom* **12**, 543–552 (1996).
37. R. G. Roberts, H. G. Yu and A. A. Maciejewski, "Characterizing Optimally Fault-Tolerant Manipulators Based on Relative Manipulability Indices," *Proceedings of the IEEE International Conference on Intelligent Robots and Systems*, San Diego, CA, USA (2007) pp. 3925–3930.
38. P. Croke, "A robotics toolbox for MATLAB," *IEEE Robot. Autom. Mag.* **3**, 24–32 (1996).
39. J. Zhao, H. Jing and L. Nie, "Motion punning based on two new fault tolerant indexes for redundant manipulators " *Chin. J. Mech. Eng.* **17**, 240–243 (2004).
40. J. Zhao and Q. Li, "An Analytical Algorithm with Minimum Joint Velocity Jump for Redundant Robots in the Presence Of Locked-Joint Failures," *Proceedings of the IEEE International Conference on Robotics and Automation*, Pasadena, CA, USA (2008) pp. 1987–1992.

https://doi.org/10.1017/S0263574711000671 Published online by Cambridge University Press